European Journal of Orthopaedic Surgery & Traumatology
https://doi.org/10.1007/s00590-019-02530-3

ORIGINAL ARTICLE • HIP - BIOMATERIALS

A porous polymeric–hydroxyapatite scaffold used for femur fractures treatment: fabrication, analysis, and simulation

Saeid Esmaeili[1] · Hossein Akbari Aghdam[2] · Mehdi Motiffard[2] · Saeed Saber-Samandari[1] · Amir Hussein Montazeran[1] · Mohammad Bigonah[3] · Erfan Sheikhbahaei[4] · Amirsalar Khandan[1]

Received: 11 January 2019 / Accepted: 9 August 2019

Abstract

Background One of the most common fractures in the skeleton happens in the femur. One of the important reasons for this fracture is because it is the longest bone in the body and osteoporosis affect this part a lot. The geometric complexity and anisotropy properties of this bone have received a lot of attention in the orthopedic field.

Methods In this research, a femur designed using 3D printing machine using the middle part of the hip made of polylactic acid–hydroxyapatite (PLA–HA) nanocomposite containing 0, 5, 10, 15, and 25 wt% of ceramic nanoparticle. Three different types of loadings, including centralized loading, full-scale, and partially loaded, were applied to the designed femur bone. The finite element analysis was used to analyze biomechanical components.

Results The results of the analysis showed that it is possible to use the porous scaffold model for replacement in the femur having proper strength and mechanical stability. Stress–strain analysis on femoral implant with biometric HA and PLA after modeling was performed using the finite element method under static conditions in Abaqus software.

Conclusion Three scaffold structures, i.e., mono-, hybrid, and zonal structures, that can be fabricated using current bioprinting techniques are also discussed with respect to scaffold design.

Keywords Bone · Hydroxyapatite · Finite elements analysis · Static and dynamic analysis · 3D printing · Femur · Fracture

Introduction

The human body has a complex architecture of organs and tissues with a distinct function. As the age rises, many changes occur in the body, which can damage the tissues or impair their normal function. One of the most important organs in the human body is bone tissue and bone stability [1]. The bones are composed of collagen fibers and crystals of hydroxyapatite (HA). The most important element of our skeletal system is bones having a ceramic and polymeric part. Bones have different mechanical and metabolic functions in our bodies. Anisotropic bones (mechanical properties vary in different directions), as they maintain the skeletal framework of our body, allow the transmission of sound in the ear and flow of blood through the bodies and vessels in the bone marrow [2, 3]. These functions have serious implications for the mechanical properties of the bones after years [4, 5]. For example, bones should be rigid enough to tolerate the body weight and also be tight enough not to break easily. During the life of the bones, many changes may occur due to events throughout the life, e.g., becoming osteoporotic. One of the most common events is hip fractures, which are divided into different types. Bone marrow grafts are divided into several categories like autograft, allograft, and animal donation [4]. During the recent years, doctors have been investigating the treating patients with large and complex fractures, but nevertheless each has a negative aspect using artificial bone like weak mechanical features. For this reason, in recent years, many scholars have focused their studies on the use of biocompatible materials with suitable chemical and mechanical properties cultured with cells and growth

✉ Amirsalar Khandan
sas.khandan@aut.ac.ir

[1] New Technologies Research Center, Amirkabir University of Technology, Tehran 15875-4413, Iran

[2] Department of Orthopedic Surgery, School of Medicine, Isfahan University of Medical Sciences, Isfahan, Iran

[3] Mechanical Engineering Department, Iran University of Science and Technology, Tehran, Iran

[4] Student Research Committee, School of Medicine, Isfahan University of Medical Sciences, Isfahan, Iran

Published online: 16 August 2019

factors to repair damaged bones [5–7]. Resorbable bio-nanocomposite containing PLA has expanded a large application in clinical fields over the whole body. These applications can be used in multiple head surgeries for craniofacial anomalies (e.g., enophthalmos) and trauma-induced fractures (orbital floor or mandibular defects); sutures and anchoring the tendons to the bones (e.g., rotator cuff or Achilles tendon repair); interference screw (e.g., anterior cruciate ligament repair); plates for fractures (e.g., distal radius or chest wall stabilizer); filling the defects after removing the cancerous bone (osteosarcoma, Ewing sarcoma, etc.); regenerative medicine (e.g., in cartilage and meniscus repair); and vascular stents. The artificial scaffold plays a key role in the process of bone repair and is usually made of degradable materials that can gradually degrade with the passing of time. A bony scaffold must have a good mechanical strength to withstand the forces involved in the atomic microscopy. The common methods for making porous the bone scaffold are using space holder technique, freeze drying, electrospinning and advanced 3D printing method [8–12]. Nowadays, the 3D printing method used for porous bio-nanocomposite scaffolds has attracted an effective reflection in scientific societies, but they have some limitations like using ceramic matrix composites. It is essential to measure the stiffness in the part of the bone without intervening other parts of the hierarchical structure [13–18]. The advance of numerical methods leads the researchers to check the performance of scaffolds using the finite element method (FEM) based on the CT scan data. Using micro-CT scan data to accurately simulate the internal structure of scaffold performed by Yang et al. [14]. In addition to the fact that the properties of a bone vary in different places, for example, the femoral neck region has a rigidity of about 6.9 GPa, while the shaft cortex holds 25 GPa as a long bone. In the middle section of the bone with low stiffness, a crack grows easily, and therefore it is more under stress. In this paper, the study focused on the preparation of biocompatible porous bony part using three-dimensional (3D) printers with a combination of polylactic acid (PLA) polymer and HA nanoparticles as an enhancer. Finally, the mechanical and biological properties of porous scaffolds were assessed.

Materials and methods

Design and fabrication of composite filament

The fabrication of a scaffold with a filament containing bio-nanocomposite ceramic composed of PLA polymer materials is performed in this research. At first, we designed a composite filament to insert in the 3D printer. Then, scaffolds were modeled by a computer and printed using FDM (fused deposition modeling) printing machine. The standard filaments with 1.75 (mm) diameter were fabricated using an extruder having a suitable heater that is turned on to preheat the extruder tubes. In order to make the filament, the extruder mold was designed and made to fit the diameter, and the heater of the machine was turned on to preheat the extruder tubes. The proper speed for the roundabout of the worm gear as well as the filament torque was adjusted, and the filament winding fan was ready to work. To make a PLA–HA bio-nanocomposite filament, a different weight percent (wt%) of hydroxyapatite (CAM Netherlands with microcrystalline particle size less than 100 nm (nm) and 98% nanocrystalline purity) with 5, 10, 15, and 25 wt% was mixed with PLA-heated granules and ground for 20 min on magnetic stirrer. After passing through the extrusion molding, the filament struck toward the fatal and collector. The operation continued until all the material was finished. A porous cylindrical scaffold having circle morphology on the body was designed using SolidWorks software. The shape of the microstructure was adjusted to a cylindrical size of 20 mm in diameter and a height of 20 mm for a relative proportional mass with large human bone implants. The symmetric design was considered with various heights regarding having a better repulsion in vertical forces. The distance between each porosity in the shape of the walls was considered to be 2–3 (mm). After completing the design, the model was inserted into the STL format and entered into the 3D software to perform the printer settings. In the software environment, the settings for the low-temperature exhaust outlet of the printer were set to 215 °C and the nozzle diameter was 0.3 mm. Finally, the layer was set to 200 microns, and the simulation of the 3D printer, as well as the G-code output for the device, was made. Finally, the codes were transmitted to the printer and the device was prepared for printing. After leveling, calibrating, and adjusting, the extruder's temperature is set at 215 °C. Then, the process of printing began and the construction of each piece took about two hours. Figure 1 shows the process of designing a porous composite containing ceramic nanoparticles in a polymer structure in a 3D printer.

Mechanical testing of porous bony scaffold

The mechanical properties of the scaffolds were measured using a compressive strength test device (SANTAM-STM50, New Technology Research Centre, Tehran, Iran). For this purpose, each sample was loaded at a rate of 0.2 mm/min and the tensile strength was evaluated. The output of the device, which was the force and displacement data, became strain due to the diameter and initial length of each sample. Finally, by using the gradient of the elastic region of the stress–strain curve, the elastic modulus of each sample was obtained. Also, the highest point in the graph shows the highest stress tolerated by the sample that was considered

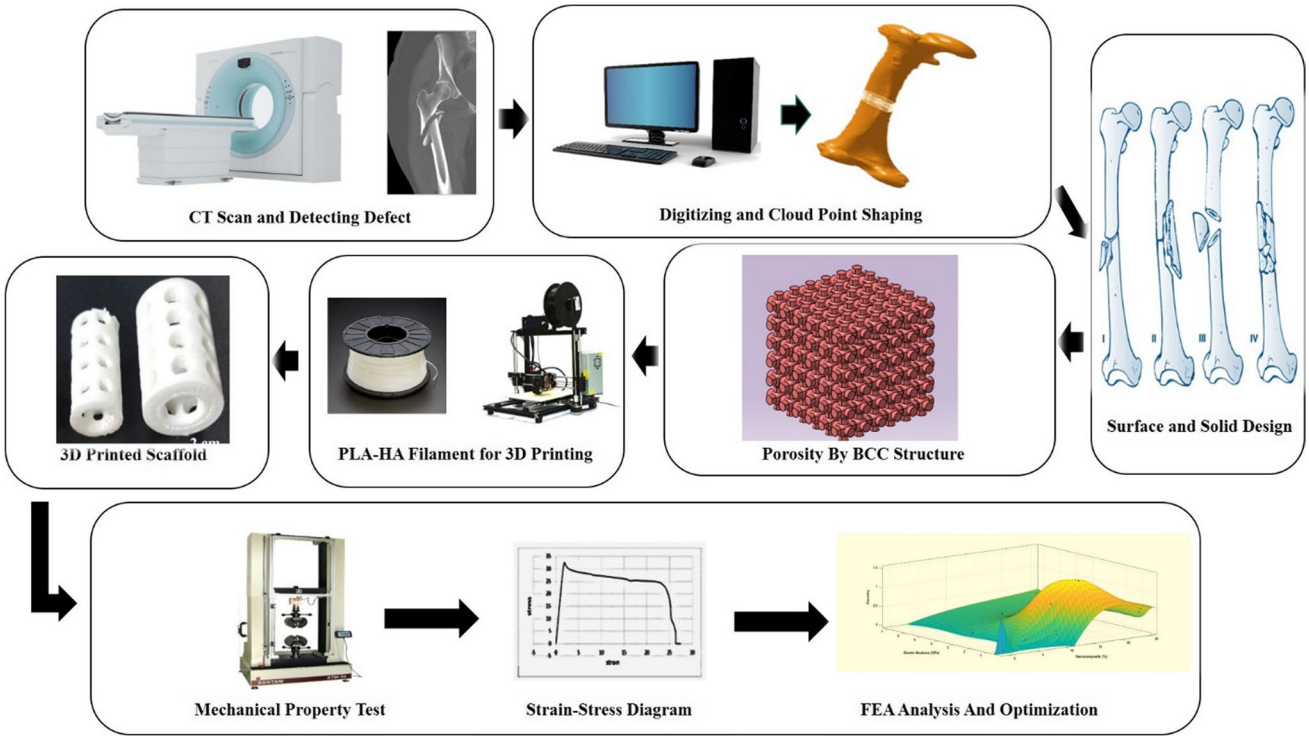

Fig. 1 Schematic of fabrication of 3D-printed porous bony scaffold made of PLA–HA bio-nanocomposite using FDM technology

as the compressive strength of the sample. After that, the rigidity test and the Young's modulus were tested using the tensile strength machine.

Porosity testing of porous bony scaffold

For calculating the porosity and density of scaffolds, the samples were submerged in the ethanol according to the Archimedes principle. The density measurements provided information on the size and distribution of pores, permeability, and structural imperfections in the produced sample. In this method, regarding high hydrophobicity of the polymer, instead of water, 96% ethanol was used to penetrate easily into small porosities. The density of the scaffold (ρ) is calculated from Eq. (1):

$$\rho = W/V_2 - V_3. \tag{1}$$

Also, the amount of open porosity of the scaffold (ε) is obtained from Eq. (2):

$$\varepsilon = V_1 - V_3/V_2 - V_3, \tag{2}$$

in which W is the scaffold weight, V_1 is the volume of ethanol in the cylindrical tube, V_2 is the volume of ethanol after placing the sample in a cylindrical tube for 5 minutes, V_3 is known as the remaining volume of ethanol after removing the specimen from the tube. The value $(V_1 - V_2)$ represents the size of the scaffold, and the $(V_1 - V_3)$ shows the volume of the absorbed ethanol. Therefore, the final volume of the scaffold is in accordance with the following:

$$V = \left(V_1 - V_2\right) + \left(V_1 - V_3\right).$$

The simulated body fluid (SBF) is replaced after 24 and 72 h and was replaced every week. It should be noted that at all stages until the fourth week, the pH of the solution should be kept at a yield of 7.2–7.4. The scaffolds are incubated for 4 weeks at 37 °C.

Modeling and analysis

FDM is a numerical method for solving the approximate differential equations and solving integral equations. The fundamental of this work is the simplification of complex differential equations for ordinary differential equations, which can be solved by numerical methods such as Euler. In solving partial differential equations, the key problem is that the error in the initial data and during the solution is not enough to result in inaccurate results. There are methods with various advantages and disadvantages for this solution, in which the finite element method is one of the best techniques to solve these problems. This method is very useful for solving partial differential equations on complex domains. There are several softwares available in this field, such as Abaqus software, to model a cylinder with a radius of 20 mm and a height of 20 mm such that the dimensions of its cavities are

2 mm apart. Young's modulus, Poisson's coefficient, and density were considered according to Table 1 for different weight percentages of additives. The load was changed from 10, 100, 1000, to 10,000 (N), corresponding to various static and dynamic loads.

Results

Mechanical evaluation of porous cylindrical bio-nanocomposite

Figure 1 represents the fabrication process of the porous cylindrical shape with circle morphology using FDM technique with PLA and HA powders. The femoral bone fracture was detected using CT scan photograph. Then, the CT micrograph was inserted into the solid work using Mimics software. Then, the produced filaments were inserted into 3D machine to build the prospective architecture. Figure 2a, b shows the designed small, medium, and big cylindrical architectures having the circle shape from top and lateral view. Before performing any Abaqus analysis on the femoral bone, it should be ensured that the mechanical response of the model under loading is comparable to the actual bone.

In order to investigate the mechanical response of the model and compare it with the actual bone, the model was placed under the loading conditions imposed by Cristofolini et al. [25] works on the true bone and tibia bone composite. The combination of two types of bending and compression loading on bone produces a transverse fracture, and the pressure causing the fracture of the beam regarding the Abaqus analysis is shown in Fig. 3. Figure 3a–f shows that as the Young modulus of the samples increased, the neutral warp approaches the center of the bone and the stresses in the nodes increased. The following reason reduces the probability of shielding stress. As it was seen, in the case of plain plated surfaces, in almost all areas, the stress levels were larger than the other plaques. The samples were broken under axial load at an angle of 30°–40° due to high shear force and the available crack in the cavities. However, according to this study the microscopic and physical nature of this type of fracture occurs on the side of the neutral axis that occurs in the tensile or compression as shown in Fig. 4a. The results obtained in the static analysis shows that the maximum stress produced at the load of 100 N concentrated at 56–58 megapascal (MPa), while at a 1000 N load the sample goes to the plastic region.

Table 1 Young's modulus, Poisson's coefficient, and compressive strength of porous bio-nanocomposite containing PLA and ceramic nanoparticles with different weight percentages made by three-dimensional printing technology

Material properties	Poisson ratio	Elastic modulus (GPa)	Density (g/cm^3)	Compressive strength (MPa)	Porosity (%)
PLA	–	–	–	35	85
PLA-5 HA	0.30	3.6	1.1	42	75
PLA-10 HA	0.33	4.2	1.5	48	79
PLA-15 HA	0.34	5.6	2.0	56	73
PLA-25 HA	0.35	6.9	3.0	58	64

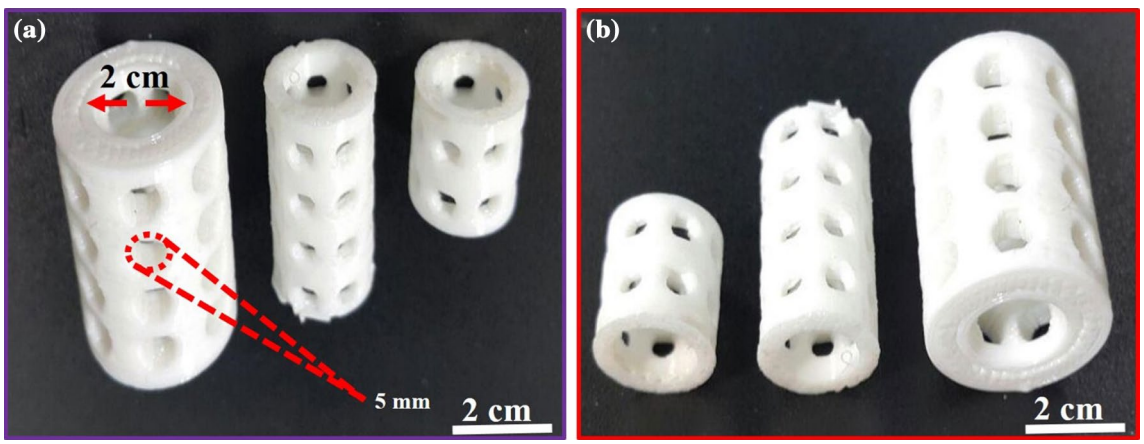

Fig. 2 3D-printed porous bony architecture in various sizes from **a** top, **b** lateral view designed using FDM process

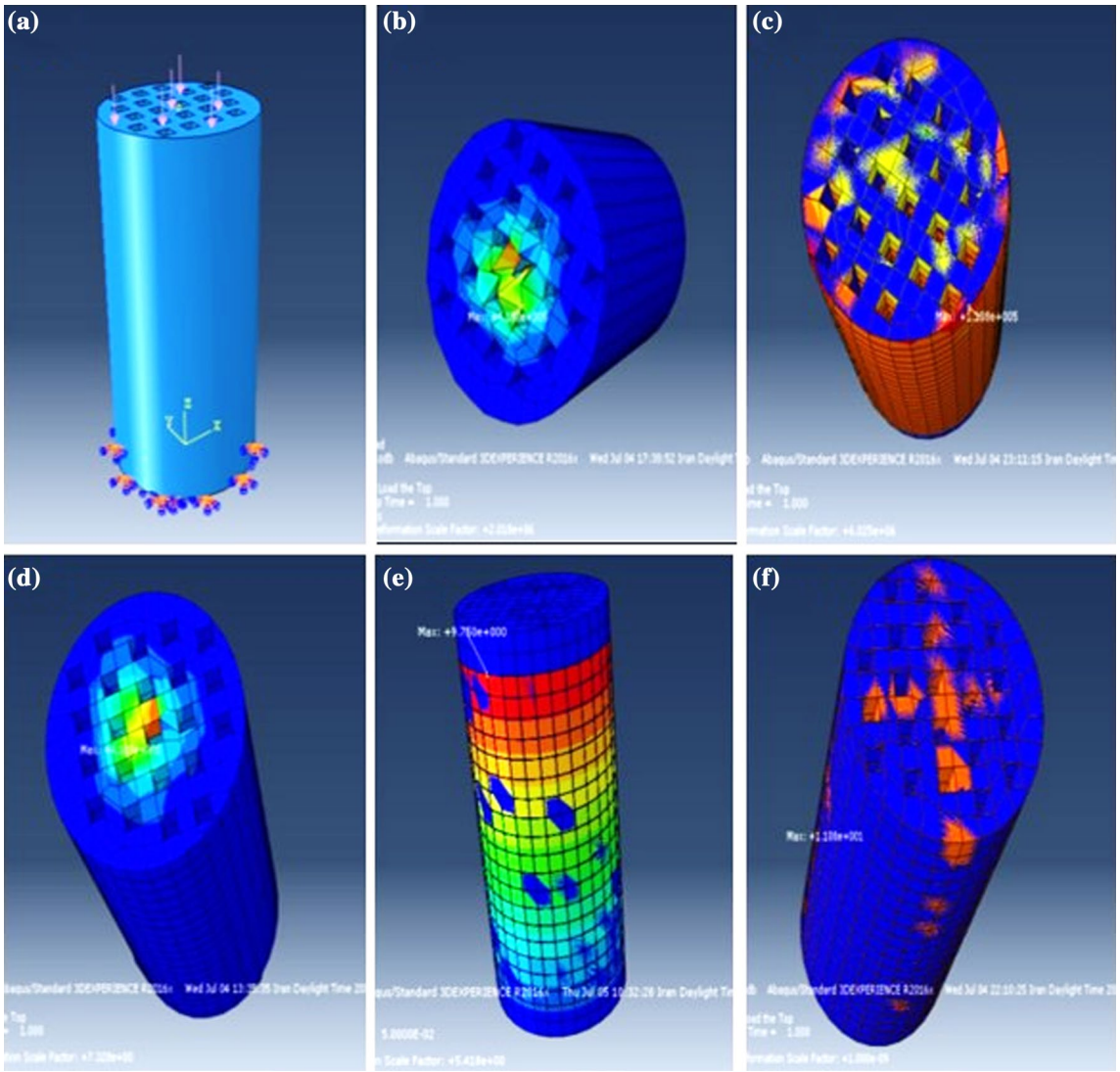

Fig. 3 Different loadings on bone scapular samples with 30 wt% weight percentages of hydroxyapatite

Discussion

Failure generally occurs in the spongy bone more than the compact bone regarding their higher mechanical properties. Figure 4a, b shows the compressive strength of samples increased from 35 to 58 MPa, while the elastic modulus increased more than two times with adding dense bioceramic materials. Also, the porosity value decreased as the addition of reinforcement increased from 0 to 25 wt%. The variation of scaffold CS is within 3–5 MPa. The comparison between porosity percentages and CS value indicated that sample with 25 wt% of HA has a close correlation between porosity value and CS value.

The above combination of proper mechanical properties and chemical stability promotes the rigidity and resistance of the bone to any external or axial load. According to the results of this research, the outcome shows that the bone strength with lower porous architecture decomposes energy without forming large cracks that cause fracture and failure.

Figure 5a–d represents the 3D curve of the optimum spot for the samples with changes in the reinforcement amount. The Young modulus of the specimen is derived from the stress–strain at static or dynamic load due to the loading rate. Then, the obtained result with SD $\pm$ 3 has several points and results for modulus of elasticity for porous microstructure. Using optimization theories and interpolation, the results were simulated and are shown in Fig. 5a–d. Both optimization and experimental results showed that mechanical properties are a function of the porosity and the effects of density on the mechanical properties of the samples were tangible. However, the real porous bone contains collagen with connective tissue property that disjoints clustering characteristic

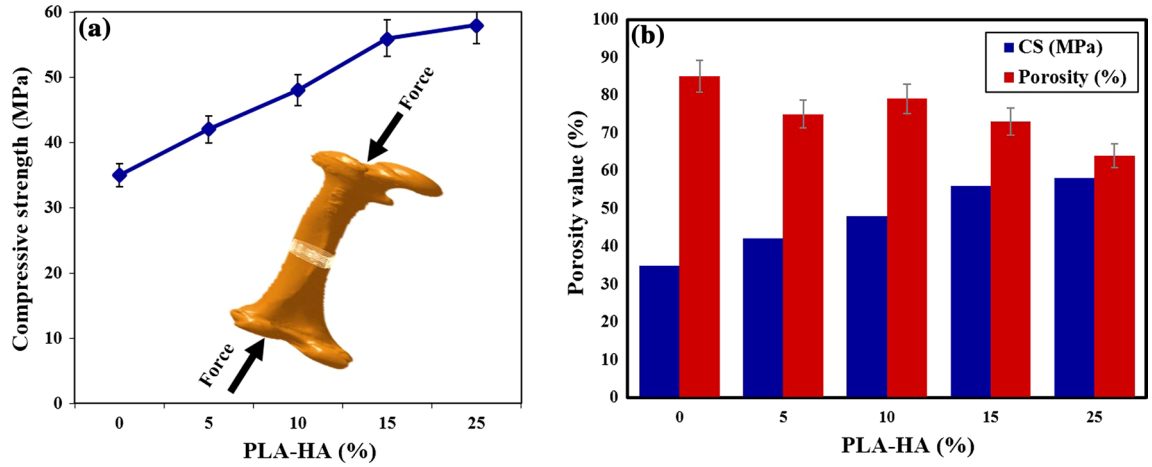

Fig. 4 **a** Compressive strength value of porous bony scaffold containing 0, 5, 10, 15, 25 wt% HA in PLA polymer, **b** comparison of porosity value versus compressive strength value under 1000 N force

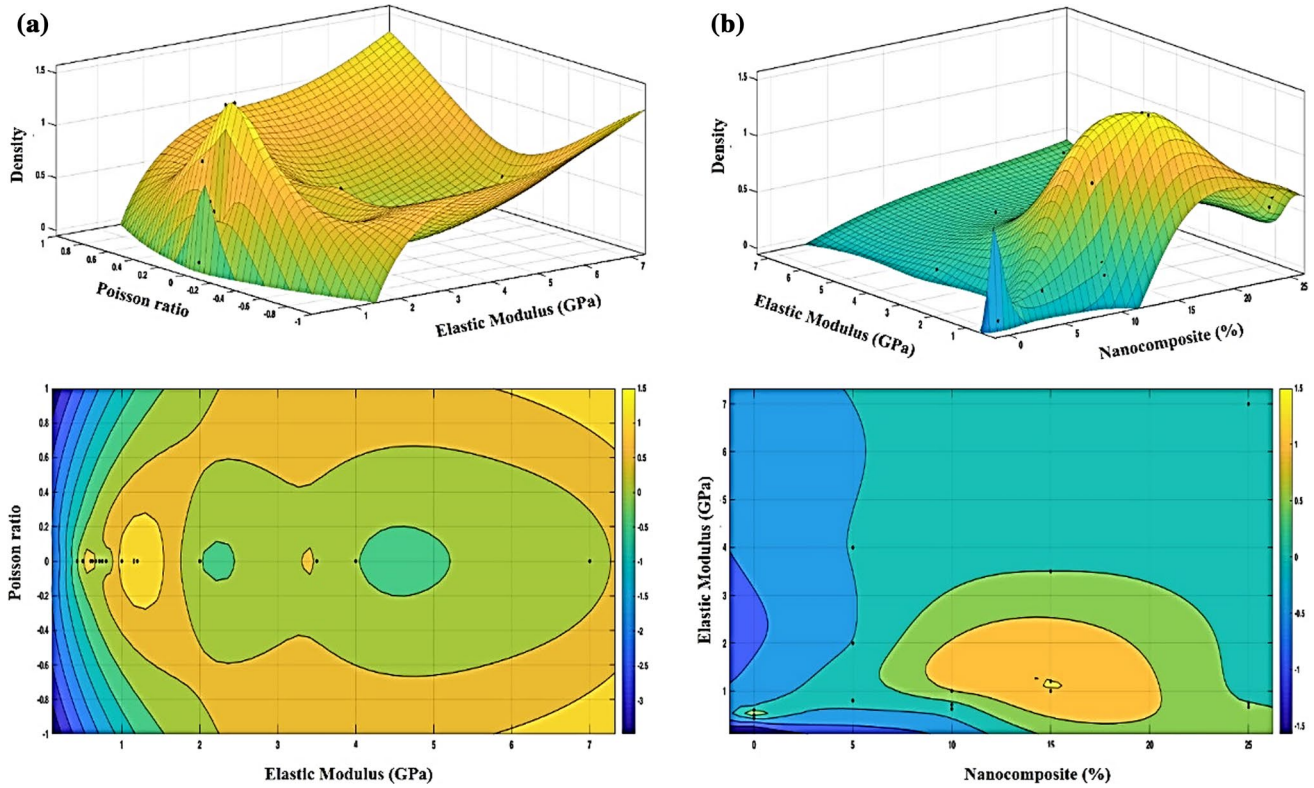

Fig. 5 Optimization of data using interpolation analysis to find the optimal effect of density changes on Poisson's coefficient, Young's modulus, and weight percentage

and leads the bone to have varied mechanical behavior under loading conditions. It should be noted that the fracture in the bone occurs in a region with a density and a large volume of spongy architecture as shown in Fig. 5a–d.

The in vitro evaluation test, after removing the scaffold from the SBF solution, showed that the amount of calcium absorption was increased after 28 days for the sample with 15 wt% HA. The reason is that the higher percentage of calcium ion in the solution is carried out more by the lower porous scaffold. As shown in Fig. 6a, the specimen containing 25 wt% had the highest apatite formation. In

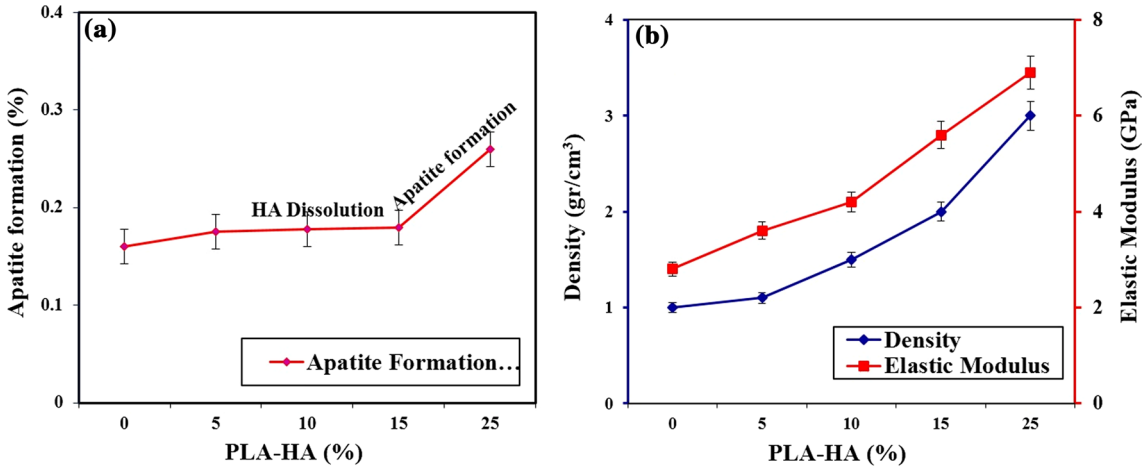

Fig. 6 **a** Apatite formation, **b** variation of density versus elastic modulus of the samples containing various amounts of HA in PLA

this work, the density value increases with the addition of additive, while the porosity value decreased.

In addition, one of the prominent features in the properties of bone failure is the fracture toughness along collagen fibers. However, in this article the presence of collagen is assumed to be distributed homogenized. The failure in the direction of the perpendicular to the surface is twice. Therefore, the cracks in the fibrils are more easily released. This dependence of the properties of failure in the direction of collagen shows that the organic properties of bone composites have a significant effect on the fracture toughness while the torque is created inside the microstructure [19, 20]. Maximum shear stress occurs at parallel and perpendicular to the neutral axis. The maximum stresses of the compressive and tensile forces occur on the diagonal plates with the neutral axis [21–25]. The object held shear loading for angular deformation; when the material was under compression or tension loading, shear stress was also occured. The mechanical properties of bio-nanocomposite porous bone substitute, such as mechanical fracture, elastic modulus, and fracture toughness, were investigated in several researches [26–29]. The bio-nanocomposite reinforced with zinc oxide, copper oxide, carbon nanotube (CNT), diopside, magnesium oxide (MgO), and magnetite nanoparticles (MNPs) was evaluated for vibrational and bending strength of the part used for various orthopedic and bone applications [30–39]. The micromechanical model of bio-nanocomposite was investigated using Dewey and Gibson theories for orthopedic approaches used in bone trauma surgery as in vitro and in vivo study [40–46].

The calcium-rich formation is the first structural change that occurs with the HA dissolution in SBF solution as a result of the integration of the HA surface with the calcium ion present in the SBF liquid surrounded by PLA-agglomerated particles. Considering changes in the Ca/P ratio, we see that the calcium-rich formation is the result of the integration of the HA surface with the SBF of calcium ions. A 3D composite containing PLA polymer with 25 wt% HA ceramic nanoparticles can produce a good bioavailability and mechanical properties according to Fig. 6a, b. In addition, HA is capable of binding to the adhesion and growth of bone marrow cells in bone spasms. However, in this paper, 3D printing method was used due to the high mechanical properties and the percentage of optimal porosity (which is 80–85% for ceramic scaffolds). Polymer–ceramic base scaffolds have the modest mechanical strength and can be used alone in bone remodeling.

Therefore, it is better to increase and optimize the mechanical properties of biodegradable polymers scaffolds that can reduce the number of surgical operations and also reduces the recovery time of the injured member. The alteration of biodegradability that might be reducing or increasing the amount of porous bone marrow bursts resulting from polymer degradation influences on mechanical strength. Clinical applications of these biocompatible composites are evident in the field of orthopedic oncology and trauma surgery. Few types of bone cancers, e.g., Ewing sarcomas, high-grade osteosarcoma, and high-grade chondrosarcoma or any other types in which a large part of the bone has to be resected and there is a bone gap left after removing the lesion are another potential application of these bone substitutes. Furthermore, in high-energy traumas, the bone breaks into many pieces and it is hard to be assembled again; therefore, bone grafts are applicable in these cases too. Although this is a primary research in this field and a lot of strong evidences are needed, according to our results, PLA–HA bio-nanocomposites, which were designed by 3D printing, and compared to natural behavior of femur, are a good substitute for femur parts lacking sufficient healthy bone tissue to build other parts.

Conclusion

A PLA–HA bio-nanocomposite was fabricated using 3D printing machine as femoral bone for the middle part of the hip containing 25 wt% of ceramic nanoparticle. Three different types of loadings, including centralized loading, full-scale, and partially loaded, were applied to the femoral bone. The results of the analysis showed that it is possible to use the scaffold model for placement in the body as a femoral bone. According to the results of the porosity, the percentage was calculated about 80–85%. Moreover, the increase in HA content did not have a significant effect on the porosity of the samples. According to the results, the mechanical properties of HA-enhanced samples are better than the sample without HA.

Acknowledgements We acknowledge Amirkabir University Technology for their kind support throughout this research and proofreading the manuscript.

Compliance with ethical standards

Conflict of interest The authors declare no potential conflict of interests.

Ethical approval This study started after receiving its scientific ethical approval from Isfahan University of Medical Sciences that registered inquiry and funding under the No. 198091 and IR.MUI.RESEARCH.REC.1398.218 (clinical research section).

References

1. Nareliya R, Kumar V (2011) Biomechanical analysis of human femur bone. Int J Eng Sci Technol 3(4):3090–3094
2. Lengsfeld M, Kaminsky J, Merz B, Franke RP (1996) Sensitivity of femoral strain pattern analyses to resultant and muscle forces at the hip joint. Med Eng Phys 18(1):70–78
3. Saber-Samandari S, Gross KA (2009) Micromechanical properties of single crystal hydroxyapatite by nanoindentation. Acta Biomater 5(6):2206–2212
4. Fu Q, Saiz E, Rahaman MN, Tomsia AP (2011) Bioactive glass scaffolds for bone tissue engineering: state of the art and future perspectives. Mater Sci Eng C 31(7):1245–1256
5. Giannoudis PV, Dinopoulos H, Tsiridis E (2005) Bone substitutes: an update. Injury 36(3):S20–S27
6. Zaky SH, Lee KW, Gao J, Jensen A, Verdelis K, Wang Y et al (2017) Poly (glycerol sebacate) elastomer supports bone regeneration by its mechanical properties being closer to osteoid tissue rather than to mature bone. Acta Biomater 54:95–106
7. Adachi T, Osako Y, Tanaka M, Hojo M, Hollister SJ (2006) Framework for optimal design of porous scaffold microstructure by computational simulation of bone regeneration. Biomaterials 27(21):3964–3972
8. Imani M, Gooudarzi AM, Rabiee SM, Dardel M (2016) Theoretical framework for evaluating the mechanical properties of composite bone scaffolds. In: The 5th international conference on composites: characterization, fabrication and application (CCFA-5), Tehran, Iran, 20–21 Dec 2016
9. Liu X, Rahaman MN, Hilmas GE, Bal BS (2013) Mechanical properties of bioactive glass (13-93) scaffolds fabricated by robotic deposition for structural bone repair. Acta Biomater 9(6):7025–7034
10. Offeddu GS, Ashworth JC, Cameron RE, Oyen ML (2015) Multi-scale mechanical response of freeze-dried collagen scaffolds for tissue engineering applications. J Mech Behav Biomed Mater 42:19–25
11. Nikpour MR, Rabiee SM, Jahanshahi M (2012) Synthesis and characterization of hydroxyapatite/chitosan nanocomposite materials for medical engineering applications. Compos B Eng 43(4):1881–1886
12. Khandan A, Ozada N, Saber-Samandari S, Nejad MG (2018) On the mechanical and biological properties of bredigite-magnetite ($Ca_7MgSi_4O_{16}$–Fe_3O_4) nanocomposite scaffolds. Ceram Int 44(3):3141–3148
13. Tagliabue S, Rossi E, Baino F, Vitale-Brovarone C, Gastaldi D, Vena P (2017) Micro-CT based finite element models for elastic properties of glass–ceramic scaffolds. J Mech Behav Biomed Mater 65:248–255
14. Yang JP (2013) Image-based procedure for biostructure modeling. J Nanomech Micromech 4(3):B4013001
15. Pérez-Ramírez Ú, López-Orive JJ, Arana E, Salmerón-Sánchez M, Moratal D (2015) Micro-computed tomography image-based evaluation of 3d anisotropy degree of polymer scaffolds. Comput Methods Biomech Biomed Eng 18(4):446–455
16. Madi K, Tozzi G, Zhang QH, Tong J, Cossey A, Au A et al (2013) Computation of full-field displacements in a scaffold implant using digital volume correlation and finite element analysis. Med Eng Phys 35(9):1298–1312
17. Sandino C, Lacroix D (2011) A dynamical study of the mechanical stimuli and tissue differentiation within a CaP scaffold based on micro-CT finite element models. Biomech Model Mechanobiol 10(4):565–576
18. Sulong MA, Belova IV, Boccaccini AR, Murch GE, Fiedler T (2016) A model of the mechanical degradation of foam replicated scaffolds. J Mater Sci 51(8):3824–3835
19. Aghdam HA, Sheikhbahaei E, Hajihashemi H, Kazemi D, Andalib A (2018) The impacts of internal versus external fixation for tibial fractures with simultaneous acute compartment syndrome. Eur J Orthop Surg Traumatol 29:183–187
20. Salami MA, Kaveian F, Rafienia M, Saber-Samandari S, Khandan A, Naeimi M (2017) Electrospun polycaprolactone/lignin-based nanocomposite as a novel tissue scaffold for biomedical applications. J Med Signals Sens 7(4):228
21. Montazeran AH, Saber Samandari S, Khandan A (2018) Artificial intelligence investigation of three silicates bioceramics-magnetite bio-nanocomposite: hyperthermia and biomedical applications. Nanomed J 5(3):163–171
22. Joneidi Yekta H, Shahali M, Khorshidi S, Rezaei S, Montazeran AH, Samandari SS et al (2018) Mathematically and experimentally defined porous bone scaffold produced for bone substitute application. Nanomed J 5(4):227–234
23. Sahmani S, Shahali M, Khandan A, Saber-Samandari S, Aghdam MM (2018) Analytical and experimental analyses for mechanical and biological characteristics of novel nanoclay bio-nanocomposite scaffolds fabricated via space holder technique. Appl Clay Sci 165:112–123
24. Sahmani S, Saber-Samandari S, Shahali M, Yekta HJ, Aghadavoudi F, Montazeran AH et al (2018) Mechanical and biological performance of axially loaded novel bio-nanocomposite sandwich plate-type implant coated by biological polymer thin film. J Mech Behav Biomed Mater 88:238–250

25. Cristofolini L, Viceconti M (2000) Mechanical validation of whole bone composite tibia models. J Biomech 33(3):279–288
26. Maghsoudlou MA, Isfahani RB, Saber-Samandari S, Sadighi M (2019) Effect of interphase, curvature and agglomeration of SWCNTs on mechanical properties of polymer-based nanocomposites: experimental and numerical investigations. Compos Part B Eng 175:107119
27. Ayatollahi MR, Moghimi Monfared R, Barbaz Isfahani R (2019) Experimental investigation on tribological properties of carbon fabric composites: effects of carbon nanotubes and nano-silica. Proc Inst Mech Eng Part L J Mater Des Appl 233(5):874–884
28. Monfared RM, Ayatollahi MR, Isfahani RB (2018) Synergistic effects of hybrid MWCNT/nanosilica on the tensile and tribological properties of woven carbon fabric epoxy composites. Theor Appl Fract Mech 96:272–284
29. Ayatollahi MR, Barbaz Isfahani R, Moghimi Monfared R (2017) Effects of multi-walled carbon nanotube and nanosilica on tensile properties of woven carbon fabric-reinforced epoxy composites fabricated using VARIM. J Compos Mater 51(30):4177–4188
30. Khandan A, Ozada N (2017) Bredigite-Magnetite ($Ca_7MgSi_4O_{16}$–Fe_3O_4) nanoparticles: a study on their magnetic properties. J Alloys Compd 726:729–736
31. Najafinezhad A, Abdellahi M, Saber-Samandari S, Ghayour H, Khandan A (2018) Hydroxyapatite-M-type strontium hexaferrite: a new composite for hyperthermia applications. J Alloys Compd 734:290–300
32. Sahmani S, Khandan A, Saber-Samandari S, Aghdam MM (2018) Nonlinear bending and instability analysis of bioceramics composed with magnetite nanoparticles: fabrication, characterization, and simulation. Ceram Int 44(8):9540–9549
33. Sahmani S, Khandan A, Saber-Samandari S, Aghdam MM (2018) Vibrations of beam-type implants made of 3D printed bredigite-magnetite bio-nanocomposite scaffolds under axial compression: application, communication and simulation. Ceram Int 44(10):11282–11291
34. Khandan A, Karamian E, Bonakdarchian M (2014) Mechanochemical synthesis evaluation of nanocrystalline bone-derived bioceramic powder using for bone tissue engineering. Dent Hypotheses 5(4):155
35. Heydary HA, Karamian E, Poorazizi E, Khandan A, Heydaripour J (2015) A novel nano-fiber of Iranian gum tragacanth-polyvinyl alcohol/nanoclay composite for wound healing applications. Procedia Mater Sci 11:176–182
36. Heydary HA, Karamian E, Poorazizi E, Heydaripour J, Khandan A (2015) Electrospun of polymer/bioceramic nanocomposite as a new soft tissue for biomedical applications. J Asian Ceram Soc 3(4):417–425
37. Abdellahi M, Najafinezhad A, Ghayour H, Saber-Samandari S, Khandan A (2017) Preparing diopside nanoparticle scaffolds via space holder method: simulation of the compressive strength and porosity. J Mech Behav Biomed Mater 72:171–181
38. Ghayour H, Abdellahi M, Nejad MG, Khandan A, Saber-Samandari S (2018) Study of the effect of the Zn^{2+} content on the anisotropy and specific absorption rate of the cobalt ferrite: the application of $Co_{1-x}Zn_xFe_2O_4$ ferrite for magnetic hyperthermia. J Aust Ceram Soc 54(2):223–230
39. Kordjamshidi A, Saber-Samandari S, Nejad MG, Khandan A (2019) Preparation of novel porous calcium silicate scaffold loaded by celecoxib drug using freeze drying technique: fabrication, characterization and simulation. Ceram Int 45(11):14126–14135
40. Esmaeili S, Shahali M, Kordjamshidi A, Torkpoor Z, Namdari F, Samandari SS et al (2019) An artificial blood vessel fabricated by 3D printing for pharmaceutical application. Nanomed J 6(3):183–194
41. Sahmani S, Shahali M, Nejad MG, Khandan A, Aghdam MM, Saber-Samandari S (2019) Effect of copper oxide nanoparticles on electrical conductivity and cell viability of calcium phosphate scaffolds with improved mechanical strength for bone tissue engineering. Eur Phys J Plus 134(1):7
42. Sadeghpour A, Mansour R, Aghdam HA, Goldust M (2011) Comparison of trans patellar approach and medial parapatellar tendon approach in tibial intramedullary nailing for treatment of tibial fractures. J Pak Med Assoc 61(6):530
43. Rouhani A, Elmi A, Aghdam HA, Panahi F, Ghafari YD (2012) The role of fibular fixation in the treatment of tibia diaphysis distal third fractures. Orthopaed Traumatol Surg Res 98(8):868–872
44. Safari MB, Tabrizi A, Hassani E, Aghdam HA, Javad M (2017) Painful scoliosis secondary to posterior rib osteoid osteoma: a case report and review of literature. J Orthop Spine Trauma 3(1):e4903
45. Farazin A, Akbari Aghdam H, Motififard M, Aghdavoudi F, Kordjamshidi A, Saber-Samandari S, Esmaeili S, Khandan A (2019) A polycaprolactone bio-nanocomposite bone substitute fabricated for femoral fracture approaches: molecular dynamic and micromechanical investigation. J Nanoanal. https://doi.org/10.22034/jna.2019.584848.1134
46. Aghadavoudi F, Golestanian H, Tadi Beni Y (2018) Investigating the effects of CNT aspect ratio and agglomeration on elastic constants of crosslinked polymer nanocomposite using multiscale modeling. Polym Compos 39(12):4513–4523